Thermal Stability of Calmodulin and Mutants Studied by $^{1}H-^{15}N$ HSQC NMR Measurements of Selectively Labeled [^{15}N]Ile Proteins

Rodolfo R. Biekofsky,[‡] Stephen R. Martin,[§] John E. McCormick,[‡] Laura Masino,[‡] Sandrine Fefeu,[‡] Peter M. Bayley,[§] and James Feeney*[,‡]

Division of Molecular Structure and Division of Physical Biochemistry, National Institute for Medical Research, Mill Hill, London NW7 1AA, U.K.

Received December 21, 2001; Revised Manuscript Received March 11, 2002

ABSTRACT: Calmodulin, the Ca^{2+}-dependent activator of many cellular processes, contains two well-defined structural domains, each of which binds two Ca^{2+} ions. In its Ca^{2+}-free (apo) form, it provides an attractive model for studying mechanisms of protein unfolding, exhibiting two separable, reversible processes, indicating two structurally autonomous folding units. $^{1}H-^{15}N$ HSQC NMR in principle offers a detailed picture of the behavior of individual residues during protein unfolding transitions, but is limited by the lack of dispersion of resonances in the unfolded state. In this work, we have used selective [^{15}N]Ile labeling of four distinctive positions in each calmodulin domain to monitor the relative thermal stability of the folding units in wild-type apocalmodulin and in mutants in which either the N- or C-domain is destabilized. These mutations lead to a characteristic perturbation of the stability (T_m) of the nonmutated domain relative to that of wild-type apocalmodulin. The ability to monitor specific ^{15}N-labeled residues, well-distributed throughout the domain, provides strong evidence for the autonomy of a given folding unit, as well as providing accurate measurements of the unfolding parameters T_m and ΔH_m. The thermodynamic parameters are interpreted in terms of interactions between one folded and one unfolded domain of apocalmodulin, where stabilization on the order of a few kilocalories per mole is sufficient to cause significant changes in the observed unfolding behavior of a given folding unit. The selective ^{15}N labeling approach is thus a general method that can provide detailed information about structural intermediates populated in complex protein unfolding processes.

The systematic analysis and understanding of the reversible folding−unfolding processes of globular proteins have been greatly advanced by the study of relatively small proteins comprising a single structural domain, and often showing a simple two-state equilibrium between folded and unfolded forms (*1*, *2*). In many cases, such systems also show simple kinetics characterized by two rate constants, k_+ and k_- for the forward and back reaction, respectively (*3*). Multidomain proteins can also show simple transition behavior (*4*). However, they are intrinsically more likely to contain regions of different stability which can present several folding processes within the same molecule (*5*−*8*). Such autonomous folding units (AFUs,[1] reviewed in ref *9*) are operationally defined substructures of the protein that can fold to nativelike conformations independent of the rest of the polypeptide chain. Such units may contain smaller identifiable generalized structures ("foldons"; *10*, *11*). One approach to understanding the complex unfolding equilibria of a potentially multidomain protein is to identify its autonomous folding units, which in the simplest case would correspond to recognizable structural domains of the protein. Where the folding−unfolding equilibrium involves multiple AFUs, the process necessarily involves folding intermediates, and presents the challenge of identifying the folding units, and characterizing the interactions between them throughout the structural transition.

Calmodulin is a ubiquitous intracellular eukaryotic calcium signal receptor and enzyme activator, which, in its calcium-free form, is an attractive model system for studying the unfolding behavior of modular assembly proteins. Apocalmodulin (148 amino acids) is a single-chain monomeric protein without disulfide bonds, prosthetic groups, bound metal ions, or cofactors. The protein has two homologous domains, each containing a pair of EF-hands (helix−loop−helix motifs) and capable of binding two Ca^{2+} ions (Ca^{2+}-binding sites I and II in the N-terminal domain and sites III and IV in the C-terminal domain). The NMR solution structure of apocalmodulin [1CFD (*12*) and 1DMO (*13*)] indicates that the largely independent domains are connected by a flexible linkage, as was also found in the calcium complex, Ca_4−CaM (*14*). Apocalmodulin domains unfold within a temperature range accessible to aqueous solution studies, and the thermal unfolding has been studied by optical and other techniques (*15*−*18*). The stabilities of the domains in intact apocalmodulin differ significantly from those of the

* To whom correspondence should be addressed. Telephone: +44-208-959-3666. Fax: +44-208-906-4477. E-mail: jfeeney@nimr.mrc.ac.uk.

[‡] Division of Molecular Structure.

[§] Division of Physical Biochemistry.

[1] Abbreviations: 1D, one-dimensional; 2D, two-dimensional; 3D, three-dimensional; AFU, autonomous folding unit; CaM, calmodulin; CD, circular dichroism; HSQC, heteronuclear single-quantum coherence; NMR, nuclear magnetic resonance; NOESY, nuclear Overhauser effect spectroscopy; TOCSY, total correlation spectroscopy.

10.1021/bi012187s CCC: $22.00
Published on Web 05/04/2002

corresponding isolated domain fragments (*19*, *20*).

Thermal unfolding has been widely studied using physical methods that monitor changes either in overall conformation (far-UV CD and calorimetry) or in properties of key aromatic residues (near-UV CD, UV absorption, and fluorescence) taken to reflect more global properties. Such measurements generally lack detailed structural information, and are frequently limited in their ability to resolve the overlap of multiple unfolding processes. In recent years, NMR has emerged as an especially important tool for studies of protein folding because of the unique detailed structural and dynamic information it can provide about individual atoms and residues throughout the structure. NMR studies are capable of revealing precise information on substructural properties during folding−unfolding transitions. 1D ^{1}H NMR has been used for monitoring the unfolding of individual domains in numerous multidomain proteins (*7*, *21*−*24*). This approach generally relies on finding resolved resonances (e.g., aromatic signals) from each domain that do not overlap with other resonances as the unfolding proceeds. In early work, Jardetzky and co-workers used selectively deuterated staphylococcal nuclease to provide simplified 1D ^{1}H spectra for following the protein unfolding as a function of pH (*25*, *26*). The current 2D ^{1}H−^{15}N heteronuclear single-quantum coherence (HSQC) methods, with their increase in signal dispersion, readily provide a versatile approach to unfolding studies. However, complete transition curves are often difficult to extract from complex 2D spectra, since the different NMR signals tend to lose chemical shift dispersion, leading to signal clustering as protein unfolding progresses (*27*).

This work introduces a general NMR approach for studying protein unfolding−refolding processes, using ^{15}N-selective isotopic labeling to simplify 2D ^{1}H−^{15}N HSQC spectra, and to minimize the problem of signal overlap in the unfolded state. Selective [^{15}N]Ile labeling of apocalmodulin also provides NMR probes in eight positions throughout the structure, allowing monitoring of the equilibrium thermal unfolding of the individual domains. The approach is also applied to two calmodulin mutants, apo-I63G CaM and apo-V136G CaM. These mutations involve residues in position 8 of the calcium-binding loop sequences of calcium-binding sites II and IV, respectively. These highly conserved residues contribute to the hydrophobic cores of the N- and C-domains, respectively, and are involved in the structural link of the two calcium-binding sites within each domain via a short β-sheet. Both of these mutations cause significant destabilization of apocalmodulin, shown by the increased tendency toward the unfolded state of the domain carrying the mutation (*18*, *28*). These mutant proteins provide interesting models for studying the unfolding behavior of a folded domain (C- or N-domain) of calmodulin in the presence of the other, destabilized mutant domain. It is found that the monitoring of individual residues provides a basis for an unambiguous interpretation of the unfolding of native apo domains in calmodulin and its mutants. The results allow estimates to be made of the free energy of stabilization of a given folding unit due to its interaction with a neighboring unfolded portion of the calmodulin structure. In addition, they illustrate the scope of this experimental approach to obtaining detailed information simultaneously on a number of residues involved in a complex protein folding process.

EXPERIMENTAL PROCEDURES

Protein Expression and Purification. *Drosophila melanogaster* calmodulins were expressed in *Escherichia coli* and purified as described previously (*18*). Uniformly ^{15}N-labeled proteins were made by incorporating 99% ^{15}N-labeled $(NH_4)_2SO_4$ as the sole nitrogen source in the growth medium. Selectively [^{15}N]Ile-labeled proteins were prepared by incorporating 97% [^{15}N]Ile in growth medium containing a mixture of the other unlabeled amino acids (*28*). Samples used for the NMR studies were 0.77−1.20 mM solutions of protein in a 90% H_2O/10% D_2O mixture and 0.1 M KCI. The pH of the samples was adjusted to 6.8 (uncorrected for deuterium isotope effects).

NMR Spectra. ^{1}H−^{15}N HSQC spectra were recorded on a Varian 600 Inova NMR spectrometer at 5−75 °C and acquired with ^{15}N decoupling during the acquisition period. Each spectrum was collected with 256 complex data points in the t_2 dimension and 1088 complex data points in the t_1 dimension; 16 transients per FID were recorded. The ^{1}H and ^{15}N sweep widths were 7996.8 and 2431.8 Hz, respectively. Suppression of the water resonance was achieved by the Watergate method (*29*). Data were zero-filled in both dimensions to generate a final 512 × 2048 point spectrum. 3D NOESY-HSQC and 3D TOCSY-HSQC (*30*) spectra were acquired at 5 °C for the uniformly ^{15}N-labeled sample. The data sets were processed using NMRPipe and analyzed using NMRDraw (*31*) and the Felix software package (Felix98.0, Biosym Technologies, Inc., San Diego, CA). ^{1}H chemical shifts were measured from a dioxane internal standard and referenced to 5,5-dimethyl-5-silapentane-2-sulfonate (taken as 3.750 ppm from dioxane at every temperature) (*32*). The values for the ^{1}H carrier are given by [4.97 − (T − 5) × 0.01] ppm for temperatures ranging from 5 to 75 °C. ^{15}N chemical shifts are referenced to liquid NH_3 using the frequency ratio method (^{15}N/^{1}H = 0.101329118) (*32*). NMR signal assignments were made by analyzing 3D NOESY-HSQC and 3D TOCSY-HSQC spectra and by comparison with known assignments for apocalmodulin (*13*). There was no visible precipitation of protein in samples heated above 60 °C. In addition, optical spectroscopy measurements performed at concentrations comparable with those used for the NMR study show no evidence of temperature-induced aggregation phenomena (*20*). The reversibility of the temperature-dependent chemical shift changes was demonstrated by recording low-temperature HSQC spectra at different stages of the temperature study and showing that there were no spectral changes compared with the spectrum of the starting sample.

Optical Spectroscopy. Far-UV CD spectra were recorded on a Jasco J-715 spectropolarimeter as described previously (*33*). Reversible thermal unfolding was monitored at 222 nm during heating from 5 to 85 °C at a rate of ≈1 °C/min. The sample temperature was measured using an immersed thermocouple (Comark).

Thermodynamic Analysis. Thermodynamic parameters for unfolding of the N- and C-terminal domains were obtained as described previously (*20*). The parameters obtained from thermal unfolding experiments were used to calculate free energy values using the Gibbs−Helmholtz equation:

$$\Delta G_T = \Delta H_m(1 - T/T_m) + \Delta C_p[T - T_m - T\ln(T/T_m)]$$

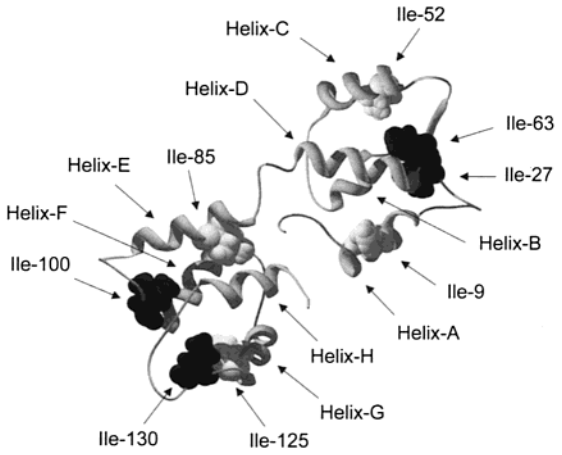

FIGURE 1: Location of Ile residues in apo-CaM [NMR average structure (1cfd); see ref *12*]. Space-filling residues colored black and gray are in loop and helical segments, respectively. The figure was drawn using Swiss-Pdb Viewer (*40*).

where T_m is the transition midpoint temperature (kelvin), ΔC_p is the heat capacity change, and ΔH_m is the enthalpy at the midpoint temperature. ΔC_p is poorly defined by the analysis and was held constant at 0.8 kcal/mol (C-domain) or 0.73 kcal/mol (N-domain) (*19*).

RESULTS

[^{15}N]Ile Selective Labeling. The thermal unfolding of wild-type apo-CaM, apo-I63G CaM, and apo-V136G CaM has been monitored using selective ^{15}N labeling of isoleucine. Of the eight isoleucine residues in CaM, four are in the N-domain, namely, Ile9 (helix A), Ile27 (site I), Ile52 (helix C), and Ile63 (site II), and four are in the C-domain, namely, Ile85 (helix E), Ile100 (site III), Ile125 (helix G), and Ile130 (site IV) (see Figure 1). The isoleucine residues are thus located in distinctive regions with different secondary structure, and pairs of residues in the sequence probe different environments, namely, the first helix and the calcium-binding loop sequence of each of the four EF-hands.

The thermal stability of the three proteins was monitored by recording 2D ^{1}H$-^{15}$N HSQC spectra at 5 °C intervals over the temperature range of 5−75 °C. The spectral simplification achieved by using selectively [^{15}N]Ile-labeled samples can be seen by comparing the ^{1}H$-^{15}$N HSQC spectra of uniformly and selectively labeled apo-CaM (Figure 2A,B). Whereas the spectrum of the uniformly labeled sample (Figure 2A) has cross-peaks for every HN moiety in the protein (~148 signals), the selectively labeled sample has just eight (Figure 2B). The denaturation of the uniformly labeled sample results in an accumulation of many signals

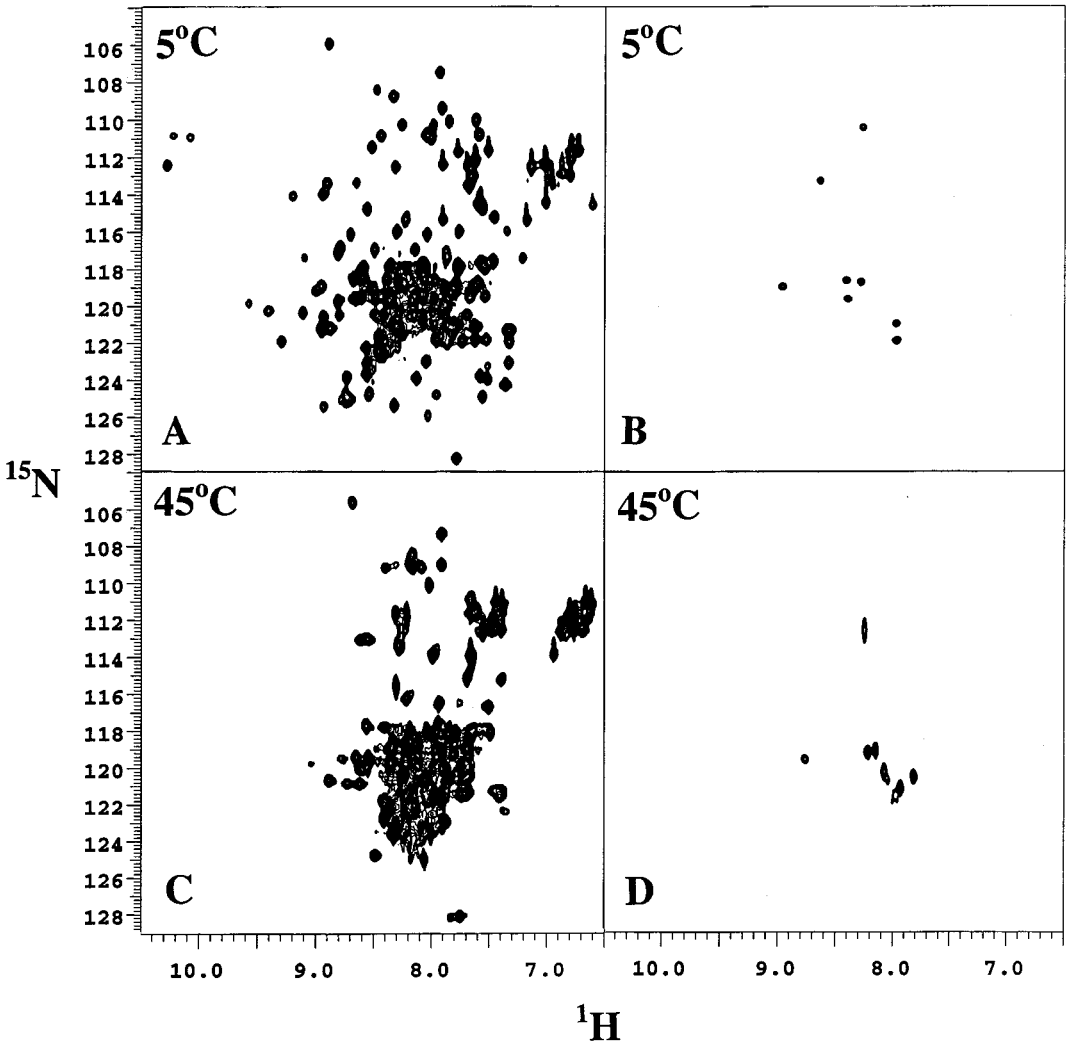

FIGURE 2: 2D ^{15}N$-^1$H HSQC spectra: (A) uniformly ^{15}N-labeled apo-CaM at 5 °C, (B) [^{15}N]Ile apo-CaM at 5 °C, (C) uniformly ^{15}N-labeled apo-CaM at 45 °C, and (D) [^{15}N]Ile apo-CaM at 45 °C.

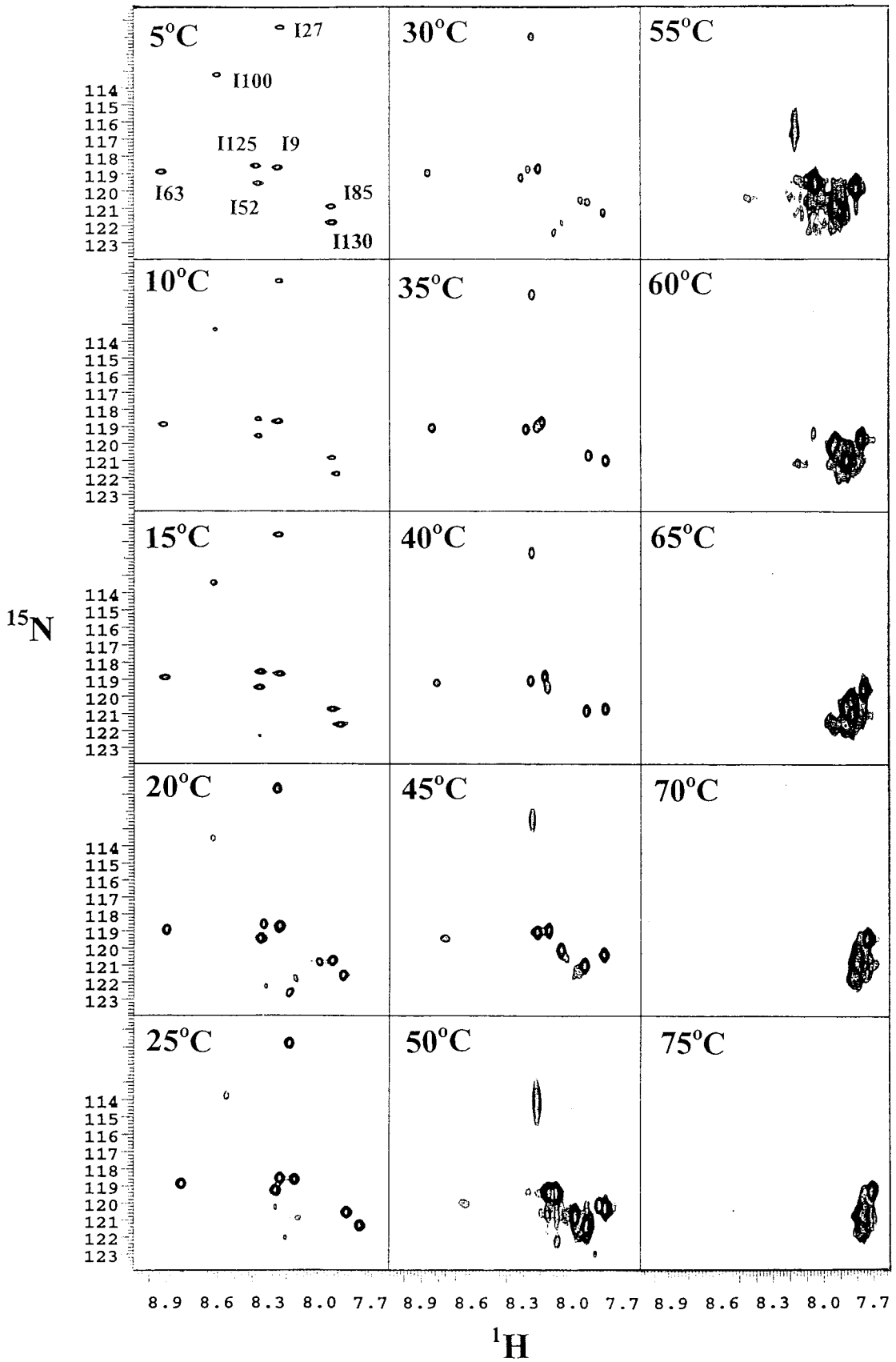

FIGURE 3: 2D ^{15}N−^{1}H HSQC spectra of [^{15}N]Ile apo-CaM at temperatures from 5 to 75 °C. Spectra from 45 to 65 °C are plotted at a very low contour level to show peaks corresponding to Ile27 and Ile63.

in the spectral region corresponding to unfolded conformations, and this prevents a quantitative analysis of the changes in chemical shift with temperature for samples approaching complete unfolding (Figure 2C). The improvement resulting from selective labeling is evident in Figure 2D.

Thermal Unfolding of Apocalmodulin. Figure 3 shows the ^{1}H−^{15}N HSQC spectra of [^{15}N]Ile apo-CaM at different temperatures. The isoleucine residues show spectral changes

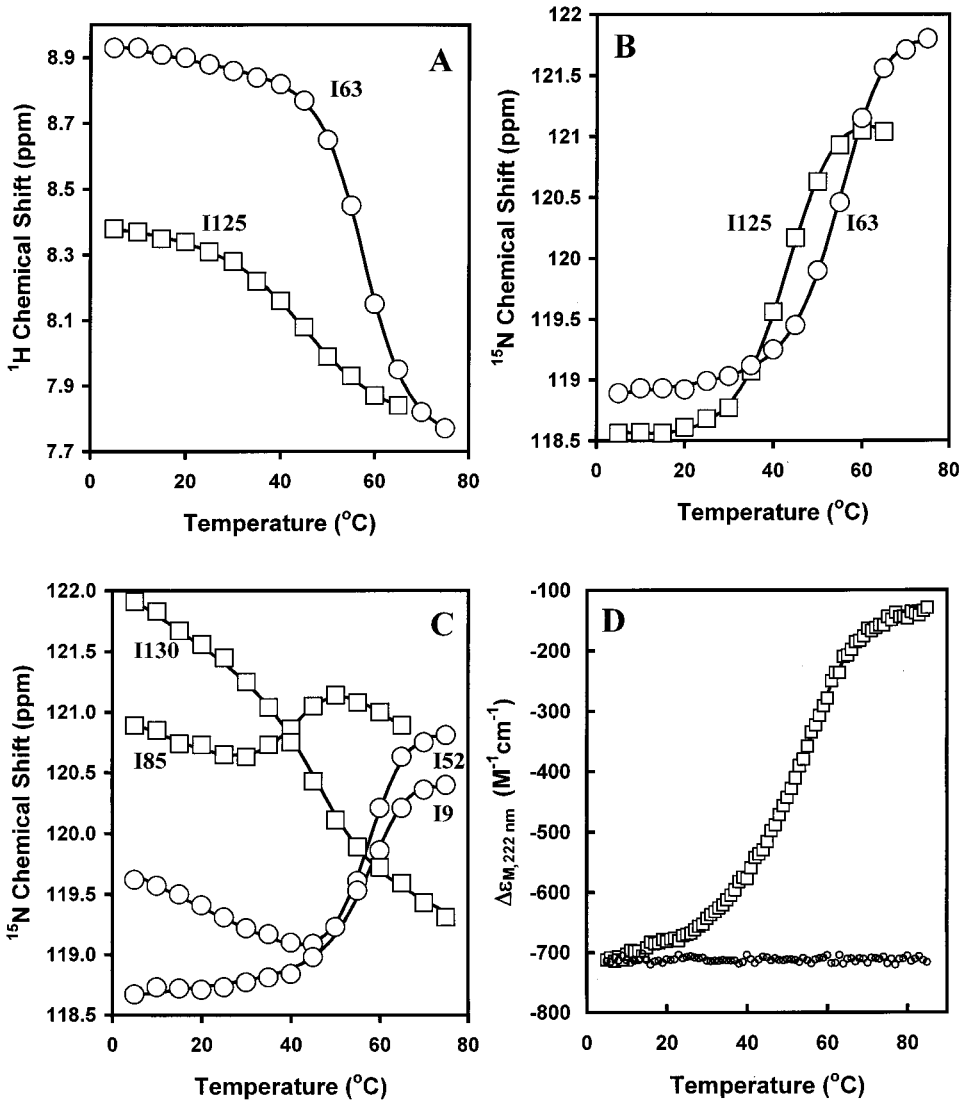

FIGURE 4: (A) ^{1}H chemical shifts as a function of temperature for residues Ile63 (N-domain) and Ile125 (C-domain) in selectively [^{15}N]-Ile-labeled wild-type apo-CaM. (B) ^{15}N chemical shifts as a function of temperature for residues Ile63 (N-domain) and Ile125 (C-domain) in selectively [^{15}N]Ile-labeled wild-type apo-CaM. (C) ^{15}N chemical shifts as a function of temperature for residues Ile9 and Ile52 (N-domain) and Ile85 and Ile130 (C-domain) in selectively [^{15}N]Ile-labeled apo-CaM. (D) Thermal denaturation of apo-CaM monitored using far-UV CD. The buffer was 25 mM MES and 100 mM KCl (pH 6.80). The solid lines are the computed best fits.

occurring in fast exchange, leading to signals with averaged chemical shifts for the nuclei exchanging between folded and unfolded species. An exception is the Ile100 signal, which disappears as the temperature increases, probably due to signal exchange broadening. For the other seven isoleucine residues, it is possible to follow the ^{1}H and the ^{15}N chemical shifts continuously as a function of temperature up to 75 °C. Panels A and B of Figure 4 show these changes for Ile63 (N-domain) and Ile125 (C-domain). Figure 4C shows the temperature dependence of the ^{15}N chemical shift for four further isoleucine residues. These plots clearly show that the unfolding of the C-domain occurs at a lower temperature than unfolding of the N-domain, and this effect is further characterized by the results of the thermodynamic analyses (Table 1).

Although the errors in the values of T_m and ΔH_m are substantial, the thermal transitions reflected by signals from isoleucine residues within a particular domain are effectively the same for residues in loops and helices. Relaxation experiments on apo-CaM (*34*) and on the apo-C-domain fragment (*35*) have shown that the Ca^{2+}-binding loops, linker, and terminal sequences are more flexible than the helices. It thus appears that the chemical shifts of HSQC signals from an isoleucine in a particular domain are relatively insensitive to the dynamics of the local structural environment.

The far-UV CD thermal unfolding curve of apo-CaM was measured under the same ionic conditions as the NMR experiments (pH 6.8 and 100 mM KCl) (see Figure 4D). The T_m and ΔH_m values for each domain are closely similar to the values determined previously at pH 8.0 (*20*) and are consistent with those determined from the NMR experiments (see Table 1).

Thermal Unfolding of Apo-I63G CaM. The replacement of Ile63 with Gly causes the N-terminal domain of the apoprotein to be significantly unfolded at room temperature (*18*). The 2D ^{1}H−^{15}N HSQC spectra of [^{15}N]Ile I63G CaM recorded at 5 °C (Figure 5A) show C-domain signals that are well-dispersed and are in the same positions as in the wild type (Figure 5B). In contrast, the observed N-domain signals have chemical shifts very different from those of the

Table 1: Thermodynamic Parameters for the Unfolding of Individual Domains in Apo-CaM, Apo-I63G CaM, and Apo-V136G CaM Obtained by Monitoring NMR Spectral Changes for [^{15}N]Ile Residues

N-Domain

	wild type		V136G	
method	ΔH_m (kcal/mol)	T_m (°C)	ΔH_m (kcal/mol)	T_m (°C)
Ile9 (^{1}H)	43.8 (4.9)[a]	59.1 (1.2)	49.8 (6.0)	59.5 (1.6)
Ile9 (^{15}N)	49.8 (3.4)	57.5 (0.9)	39.9 (3.3)	62.0 (1.3)
Ile27 (^{1}H)	51.6 (11.5)	61.1 (1.9)	48.3 (11.5)	61.7 (2.2)
Ile27 (^{15}N)	49.7 (4.5)	56.2 (1.1)	52.9 (4.5)	55.7 (1.1)
Ile52 (^{1}H)	46.8 (6.2)	56.9 (0.8)	41.0 (4.4)	57.0 (2.2)
Ile52 (^{15}N)	45.0 (4.2)	58.3 (1.5)	45.7 (4.9)	59.6 (1.1)
Ile63 (^{1}H)	48.3 (3.6)	57.0 (0.7)	54.3 (5.5)	58.4 (0.9)
Ile63 (^{15}N)	42.7 (3.5)	55.3 (0.8)	47.2 (9.7)	57.2 (0.9)
NMR average	47.2 (3.2)	57.7 (1.8)	47.4 (5.1)	58.8 (2.2)
CD (pH 6.8)	44.6 (1.2)	57.5 (0.4)		
CD (pH 8.0)[b]	46.1	59.5		

C-Domain

	wild type		I63G	
method	ΔH_m (kcal/mol)	T_m (°C)	ΔH_m (kcal/mol)	T_m (°C)
Ile85 (^{15}N)	33.9 (6.6)	38.1 (1.2)	38.1 (5.2)	47.1 (1.4)
Ile125 (^{1}H)	28.1 (3.2)	41.9 (2.5)	39.2 (2.2)	50.3 (1.9)
Ile125 (^{15}N)	33.5 (2.9)	42.7 (1.2)	42.6 (2.8)	49.9 (1.2)
Ile130 (^{15}N)	34.1 (3.5)	42.9 (2.7)	34.1 (4.4)	51.1 (2.1)
NMR average	32.4 (2.9)	41.4 (2.2)	38.5 (3.5)	49.6 (1.7)
CD (pH 6.8)	31.2 (0.6)	43.5 (0.3)		
CD (pH 8.0)[b]	29.1	45.7		

[a] Values in parentheses are the estimated standard deviations. [b] From ref *20*.

N-domain signals in wild-type calmodulin (one of the three expected signals is not observed, probably because of exchange line broadening). The 2D ^{1}H-^{15}N HSQC spectra of [^{15}N]Ile I63G CaM recorded as a function of temperature allow monitoring of the unfolding of the C-terminal domain of this mutant. The profile is different from that of the wild-type C-domain (see Figure 6A) and shows that the C-domain is significantly more stable in the mutant protein (see Table 1).

Thermal Unfolding of Apo-V136G CaM. Val136 in the C-domain of CaM is in a position homologous to Ile63 in the N-domain. Replacement of Val136 with Gly causes the C-terminal domain to be unfolded at room temperature in the absence of Ca^{2+} (*18*, *28*). Thus, the 2D ^{1}H−^{15}N HSQC spectra of [^{15}N]Ile V136G CaM recorded at 5 °C (Figure 5C) show well-dispersed N-domain signals in the same positions as for wild-type calmodulin (Figure 5B), and the C-domain signals confirm that the C-domain is fully unfolded. The thermal unfolding of the N-domain of this mutant was monitored as described above. The spectral changes with temperature are the same as those of the wild-type N-domain (see Figure 6B), and analysis of the curves yields similar thermodynamic parameters (see Table 1).

Estimation of Free Energies of Unfolding at 20 °C. The parameters given in Table 1, together with values for ΔC_p, enabled the calculation of stability curves (*1*) for the variation of ΔG with temperature for the N-domains (wild-type and V136G CaM) and the C-domains (wild-type and I63G CaM). These are shown in Figure 7. The two curves for the N-domain of wild-type apo-CaM and apo-V136G CaM essentially overlap throughout the temperature range, but those for the C-terminal domains of apo-CaM and apo-I63G CaM do not. All curves predict a temperature of maximum stability close to 0 °C. Urea denaturation experiments at 20 °C, performed as described previously (*20*), showed that the N-domain of apo-I63G CaM is substantially (>75%) unfolded, whereas the C-domain of apo-V136G CaM is

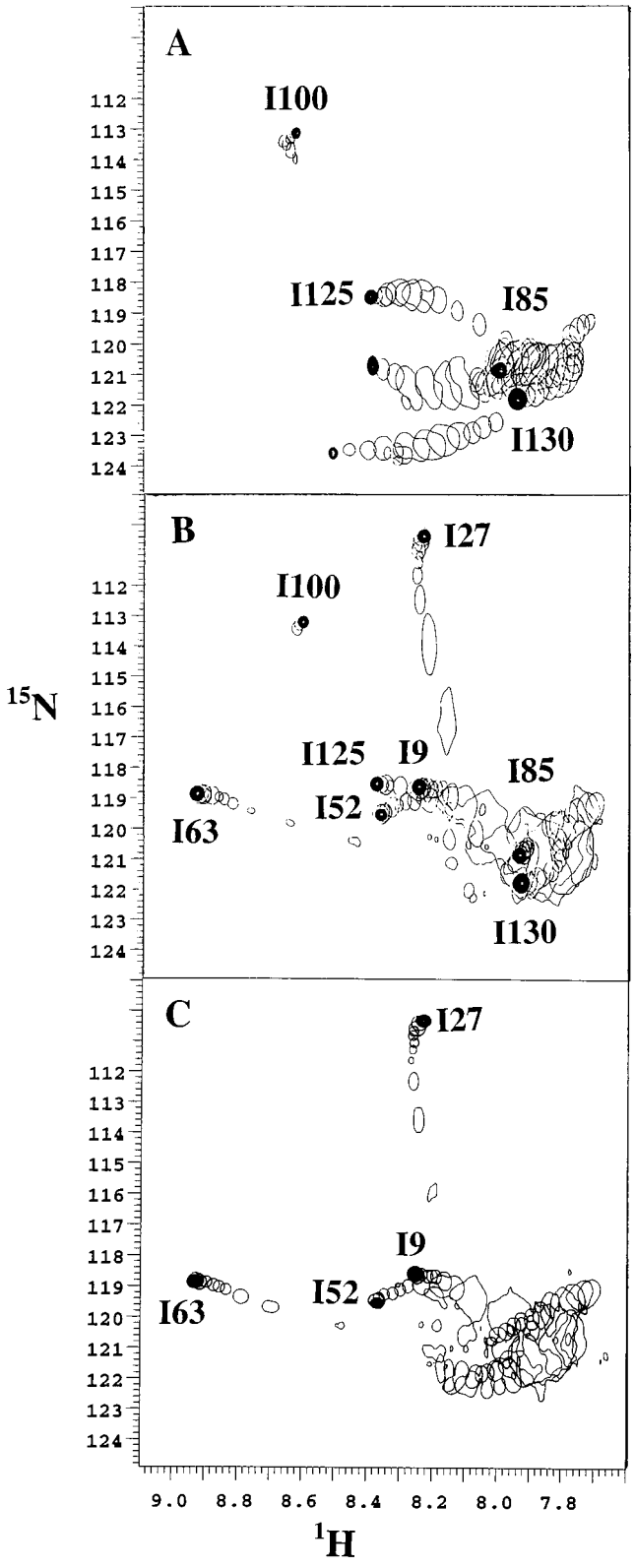

FIGURE 5: Superimposition of ^{1}H−^{15}N spectra at different temperatures for apo-I63G CaM (A), apo-CaM (B), and apo-V136G CaM (C). The initial point at 5 °C is shown by signals with full contours. Signals at higher temperatures are plotted at lower contour levels to show fast exchange averaged signals. The two unlabeled signals in panel A are from the N-domain (see the text).

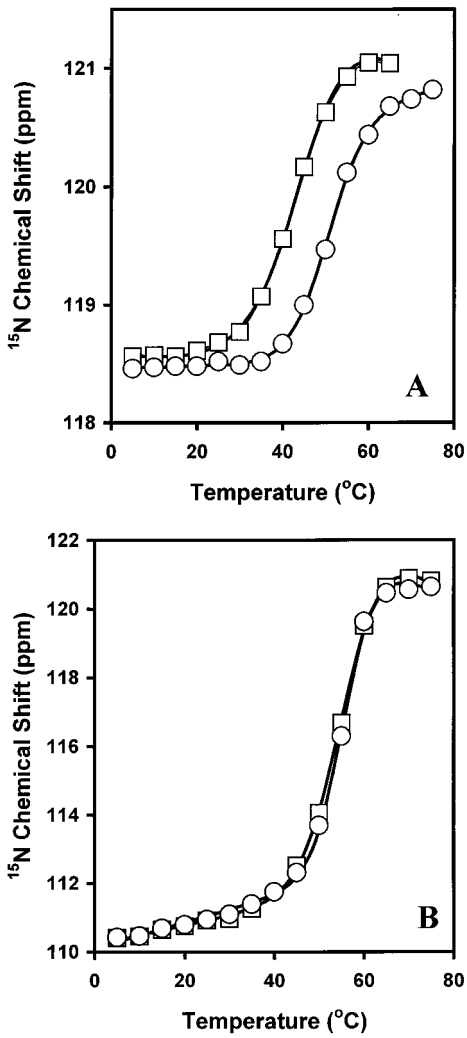

FIGURE 6: (A) ^{15}N chemical shifts as a function of temperature for residue Ile125 (C-domain) in selectively [^{15}N]Ile-labeled apo-CaM (□) and apo-I63G CaM (○). (B) ^{15}N chemical shifts as a function of temperature for residue Ile27 (N-domain) in selectively [^{15}N]-Ile-labeled apo-CaM (□) and apo-V136G CaM (○).

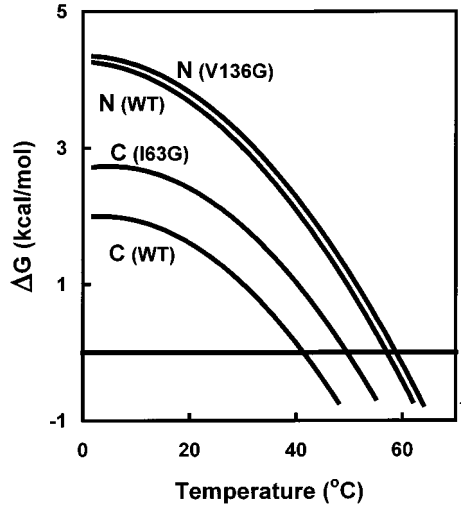

FIGURE 7: Variation of ΔG with temperature for the N-domains (wild type and V136G) and C-domains (wild type and I63G).

completely unfolded, consistent with previous observations using far-UV CD (*18*, *20*) and NMR (*28*). These experiments also allowed determination of values of ΔG_{20} for the nonmutated domains in apo-I63G CaM and apo-V136G CaM. The results are summarized in Table 2. There is generally close agreement between the NMR and CD estimates of ΔG_{20}. As has been noted elsewhere (*20*), these ΔG_{20} values are in fact quite small, so the agreement can be taken as evidence of the validity of the thermodynamic analysis. This agreement in results from two experimental regimes using protein concentrations differing by 2 orders of magnitude indicates that the reported effects do not involve intermolecular interactions.

Table 2: Comparison of Thermodynamic Parameters for Unfolding Obtained by Different Methods for Apo-CaM, Apo-I63G CaM, Apo-V136G CaM, the Isolated Apo N-Domain (Tr1C), and the Isolated Apo C-Domain (Tr2C)

		ΔG_{20} (kcal/mol)	
protein	method	C-domain	N-domain
wild type	CD-U[a]	1.45 (0.11)[b]	3.55 (0.27)
	CD-T[a]	1.43 (0.15)	3.69 (0.41)
	NMR	1.61 (0.12)	3.74 (0.31)
V136G	CD-U	na	3.82 (0.25)
	NMR	na	3.82 (0.41)
I63G	CD-U	2.24 (0.13)	na
	NMR	2.41 (0.28)	na
Tr2C	CD-U[a]	1.91 (0.12)	na
	CD-T[a]	2.22 (0.16)	na
Tr1C	CD-U[a]	na	2.73 (0.21)
	CD-T[a]	na	3.21 (0.27)

[a] Data from ref *20*. CD-U and CD-T indicate values calculated from far-UV CD urea denaturation and thermal unfolding experiments, respectively. NMR indicates values calculated from NMR thermal unfolding experiments. Values from thermal unfolding experiments were calculated using ΔC_p values of 0.8 and 0.73 kcal K^{-1} mol^{-1} for the N- and C-terminal domains, respectively (*19*). [b] Values in parentheses are the estimated standard deviations.

DISCUSSION

Interdomain Interactions between Folded and Unfolded Domains. The two domains of apo-CaM are homologous and structurally similar, comprising a four-helix bundle stabilized by a short β-strand between two antiparallel loop sequences (*12*, *13*). Nevertheless, the free energies of unfolding of the isolated domains are different (*20*). The isolated apo N-domain ($\Delta G_{20} \sim 3.0$ kcal/mol) is significantly more stable than the isolated apo C-domain ($\Delta G_{20} \sim 2.05$ kcal/mol) (see Table 2). This stability difference is not evident in the T_m values, which are very similar (50.3 and 49.4 °C for the isolated N- and C-domains, respectively). The differential effects of calcium binding on the stability of both domains have been described and quantitated elsewhere (*20*).

For apo-CaM, the individual domains in the intact protein do not have the same stability as the isolated domains; the N-domain is stabilized and the C-domain destabilized with respect to the corresponding isolated domain. This is reflected in the T_m values (57.7 and 41.4 °C for the N- and C-domains, respectively) and in the free energy values ($\Delta G_{20} \sim 3.65$ kcal/mol for the N-domain and $\Delta G_{20} \sim 1.45$ kcal/mol for the C-domain) (Table 2). The extrapolated thermodynamic parameters for intact apo-CaM determined using the NMR approach are in satisfactory agreement with these values ($\Delta G_{20} \sim 3.8$ kcal/mol for the N-domain and $\Delta G_{20} \sim 1.6$ kcal/mol for the C-domain) (see Tables 1 and 2).

The two domains of apo-CaM appear to behave independently, consistent with the flexible linker and the low isoelectric point for each domain (*12*, *13*, *34*). Interactions

between folded and unfolded domains in apo-CaM have been discussed in ref *20*, and a general mechanism was suggested whereby the interaction of a folded domain (or AFU) with an unfolded one would be expected to destabilize the domain unfolding first and stabilize the domain unfolding second. An interdomain interaction between a Ca^{2+}-loaded N-domain and an unfolded mutant C-domain has been directly observed for V136G CaM (*28*). In wild-type apo-CaM, the C-domain unfolds first; hence, unfolding of the N-domain occurs in the presence of an unfolded C-domain. The thermal unfolding of the N-domain of apo-V136G CaM (in which the C-domain is already unfolded) should therefore parallel that of the N-domain in the wild-type protein. Tables 1 and 2 show that this is indeed the case; values of the thermodynamic parameters (T_m, ΔH_m, and ΔG_{20}) for the N-domain in apo-V136G CaM are closely similar to those for the wild-type apo N-domain.

In the case of apo-I63G CaM, the C-domain unfolds in the presence of the less stable, partially unfolded N-domain. One would therefore predict that interaction of the unfolded N-domain with the C-domain would make the C-domain significantly more stable than the wild-type C-domain and somewhat more stable than the isolated C-domain. The data presented here show that this indeed is true. The T_m value for the C-domain in apo-I63G CaM is some 8 °C higher than that for the wild-type C-domain. The free energy of unfolding of the C-domain in apo-I63G CaM ($\Delta G_{20} \sim 2.30$ kcal/mol) is significantly higher than that of the wild-type apo C-domain ($\Delta G_{20} \sim 1.45$ kcal/mol) and somewhat higher than that of the isolated apo C-domain ($\Delta G_{20} \sim 2.05$ kcal/mol). The stabilization with respect to the isolated C-domain is ~0.25 kcal/mol, i.e., rather small compared to the 0.6 kcal/mol stabilization of the N-domain of apo-CaM relative to the isolated N-domain.

Figure 8 summarizes the free energy values determined for unfolding of the apo forms of intact CaM and the isolated domains. Unfolding of the intact wild-type protein occurs predominantly via the upper pathway of the cycle. Interaction between the unfolded C-domain and the folded N-domain destabilizes the C-domain by ~0.6 kcal/mol relative to the isolated C-domain and stabilizes the N-domain relative to the isolated N-domain to approximately the same extent. Studies of I63G CaM allowed determination of the free energy for unfolding of a native C-domain in the presence of an unfolded mutant N-domain. Conservation of free energy then gives an estimate of ~2.8 kcal/mol for ΔG_{20} for unfolding of a native N-domain in the presence of a folded C-domain. These results suggest that interaction between the native C-domain and the unfolded N-domain may be less significant than that of the native N-domain with an unfolded C-domain occurring in the wild type.

Intramolecular Interactions in Partially Unfolded Multidomain Proteins. These results suggest that the observed differences in T_m between the domains in the wild-type protein and the corresponding isolated domains arise mainly as a result of interactions between a folded and an unfolded domain. Such interactions may be specific or relatively unspecific. For wild-type apo-CaM, no significant chemical shift changes were observed for the [15N]Ile residues in the folded domain during the unfolding of its neighboring domain, and thus, there is no evidence that the Ile residues are directly involved in such interactions in wild-type CaM.

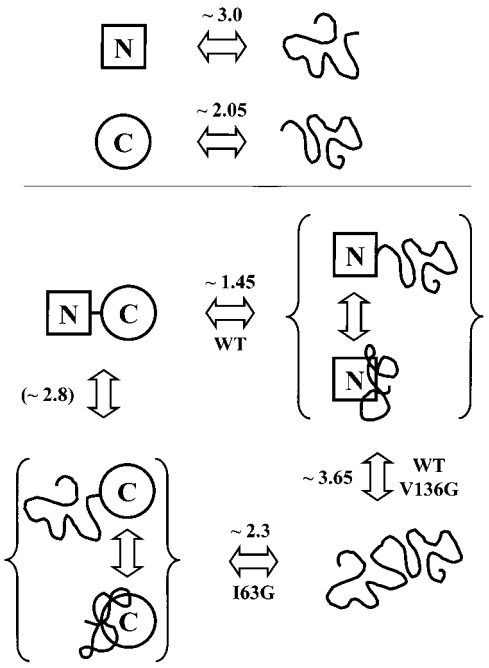

FIGURE 8: Schematic representation of the unfolding pathways for calmodulin and its isolated domains. The upper part shows the free energy values determined for the isolated fragments (*20*). The lower part shows the unfolding scheme for the intact protein with free energy values determined from experiments with the wild-type protein and the two mutants. The value for unfolding of the N-domain in the presence of a folded C-domain was determined from conservation of free energy.

The use of the β-structure mutants, apo-I63G CaM and apo-V136G CaM, provides models in which the relative stabilities of the N- and C-terminal domains are reversed by mutation. The observed change in the stability of the nonmutated domain indicates that additional stabilization of the intrinsically more stable domain can occur with either the N- or C-domain. Thus, the effect is not restricted to one domain, which excludes the likelihood that it is simply due to dividing calmodulin into two separate entities. In the case of apo-I63G CaM, two of the perturbed Ile residues in the N-domain show temperature-dependent shifts similar to those of the C-domain even though the N-domain is known, from far-UV CD measurements, to lack secondary structure. This may indicate some specificity in the interactions between the folded C-domain and unfolded N-domain. However, no such effect is seen with apo-V136G CaM.

The measurements reported here with apo-CaM and its mutants illustrate more general principles applicable to the folding−unfolding equilibria of multidomain proteins. The additional structural resolution provided by NMR is central to these deductions. The use of selective labeling of one type of residue (in this case isoleucine) at positions widely distributed in the structure provides important evidence in identifying the structure comprising the folding unit. This is particularly important when mutations are introduced into a given domain. The studies of apo-CaM presented here, with eight [15N]Ile residues distributed over its two domains with each in a significantly different secondary−tertiary structural environment, generally show a close overlap of the temperature unfolding profile for a given domain.

This result raises the question of the relationship between the overall thermodynamic stability and the structural

dynamics of the folded state of a protein domain. In the NMR studies of (folded) apo-CaM, the structure of the C-domain could not be determined to the same precision as that of the N-terminal domain because of the presence of conformational exchange occurring on an intermediate time scale of several hundred microseconds (*12*, *13*, *36*). It has been deduced from ^{15}N relaxation measurements that the apo C-domain exhibits higher conformational heterogeneity at room temperature, with significantly populated substates that have a sub-millisecond mean lifetime in the range of microseconds to milliseconds, in contrast to the apo N-terminal domain (*34*). However, the fact that three of the loop residues of calmodulin have the same unfolding profile as other labeled residues in the same domain indicates that local motion does not necessarily correlate with a reduced overall thermodynamic stability.

CONCLUSIONS

The different experimental methods used for monitoring thermal transitions of proteins have different merits, which complement one another. Optical techniques tend to be economical in materials and applicable at short time scales for kinetic work, but may lack the desired resolution. Calorimetry is highly informative for thermodynamic quantities, but lacks detailed structural information. Monitoring protein unfolding using ^{1}H−^{15}N HSQC NMR together with selective ^{15}N labeling allows the direct assignment of individual transitions to particular domains, and the measurement of thermodynamic parameters (T_m and ΔH_m) for the individual domains in a multidomain protein. This NMR approach is not restricted to equilibria in fast exchange on the chemical shift scale. For spectral changes occurring in fast exchange (as is the case for CaM), the signals have averaged chemical shifts for the nuclei exchanging between folded and unfolded states. If the spectral changes occur in slow exchange, the data analysis involves measuring the volumes of peaks representing folded and unfolded states at each temperature (*37*). In the cases of both fast and slow exchange, the method of selective ^{15}N isotope labeling helps to facilitate the data analysis by reducing signal overlap in the unfolded state. For larger proteins, selective isotopic labeling combined with the intein approach offers a potentially powerful means of isotopic labeling of selected contiguous sequences (*38*, *39*); this could enable studies of the unfolding of selected domains in >100 kDa proteins.

Apocalmodulin offers an interesting example of a protein having two homologous domains that can interact during the unfolding process, as described. This example of multidomain unfolding appears to be intermediate between the case of total (energetic and structural) autonomy of the folding of substructural units, and the more complicated case where the unfolding of the multidomain protein involves folding units which cannot be replicated by the behavior of isolated parts of the structure.

ACKNOWLEDGMENT

The NMR experiments were carried out at the MRC Biomedical NMR Centre, Mill Hill, and we thank Drs. Tom Frenkiel and Geoff Kelly for their help and advice with these experiments. We thank Prof. Kathy Beckingham (Rice University, Houston, TX) for supplying the original pOTSN-col2 vector containing the cDNA encoding *D. melanogaster* calmodulin and Peter Browne for the original cloning of the wild-type calmodulin and the I63G and V136G mutants. We thank Dr. Jens Kleinjung and Dr. Annalisa Pastore for helpful advice and discussions.

REFERENCES

1. Becktel, W. J., and Schellman, J. A. (1987) *Biopolymers 26*, 1859−1877.
2. Fersht, A. R. (1999) *Structure and mechanism in protein science: a guide to enzyme catalysis and protein folding*, W. H. Freeman, New York.
3. Jackson, S. E. (1998) *Folding Des. 3*, R81−R91.
4. Ganesh, C., Shah, A. N., Swaminathan, C. P., Surolia, A., and Varadarajan, R. (1997) *Biochemistry 36*, 5020−5028.
5. Bailey, J. M., Lin, L. N., Brandts, J. F., and Mas, M. T. (1990) *J. Protein Chem. 9*, 59−67.
6. Rudolph, R., Siebendritt, R., Nesslaüer, G., Sharma, A. K., and Jaenicke, R. (1990) *Proc. Natl. Acad. Sci. U.S.A. 87*, 4625−4629.
7. Sato, S., Kuhlman, B., Wu, W. J., and Raleigh, D. P. (1999) *Biochemistry 38*, 5643−5650.
8. Inaba, K., Kobayashi, N., and Fersht, A. R. (2000) *J. Mol. Biol. 302*, 219−233.
9. Peng, Z.-Y., and Wu, L. C. (2000) *Adv. Protein Chem. 53*, 1−47.
10. Panchenko, A. R., Luthey-Schulten, Z., and Wolynes, P. G. (1996) *Proc. Natl. Acad. Sci. U.S.A. 93*, 2008−2013.
11. Panchenko, A. R., Luthey-Schulten, Z., Cole, R., and Wolynes, P. G. (1997) *J. Mol. Biol. 272*, 95−105.
12. Kuboniwa, H., Tjandra, N., Grzesiek, S., Ren, H., Klee, C. B., and Bax, A. (1995) *Nat. Struct. Biol. 2*, 768−776.
13. Zhang, M., Tanaka, T., and Ikura, M. (1995) *Nat. Struct. Biol. 2*, 758−767.
14. Barbato, G., Ikura, M., Kay, L. E., Pastor, R. W., and Bax, A. (1992) *Biochemistry 31*, 5269−5278.
15. Brzeska, H., Venyaminov, S. V., Grabarek, Z., and Drabikowski, W. (1983) *FEBS Lett. 153*, 169−173.
16. Tsalkova, T. N., and Privalov, P. L. (1985) *J. Mol. Biol. 181*, 533−544.
17. Protasevich, I., Ranjbar, B., Lobachov, V., Makarov, A., Gilli, R., Briand, C., Lafitte, D., and Haiech, J. (1997) *Biochemistry 36*, 2017−2024.
18. Browne, J. P., Strom, M., Martin, S. R., and Bayley, P. M. (1997) *Biochemistry 36*, 9550−9561.
19. Sorensen, B. R., and Shea, M. A. (1998) *Biochemistry 37*, 4244−4253.
20. Masino, L., Martin, S. R., and Bayley, P. M. (2000) *Protein Sci. 9*, 1519−1529.
21. Bogusky, M. J., Dobson, C. M., and Smith, R. A. (1989) *Biochemistry 28*, 6728−6735.
22. Conejero-Lara, F., Parrado, J., Azuaga, A. I., Smith, R. A., Ponting, C. P., and Dobson, C. M. (1996) *Protein Sci. 5*, 2583−2591.
23. Darby, N. J., Kemmink, J., and Creighton, T. E. (1996) *Biochemistry 35*, 10517−10528.
24. Nowak, U. K., Cooper, A., Saunders, D., Smith, R. A., and Dobson, C. M. (1994) *Biochemistry 33*, 2951−2960.
25. Arata, Y., Khalifah, R., and Jardetzky, O. (1973) *Ann. N.Y. Acad. Sci. 222*, 230−239.
26. Putter, I., Markley, J. L., and Jardetzky, O. (1970) *Proc. Natl. Acad. Sci. U.S.A. 65*, 395−401.
27. Dyson, H. J., and Wright, P. E. (1998) *Nat. Struct. Biol. 5*, 499−503.
28. Fefeu, S., Biekofsky, R. R., Martin, S. R., Bayley, P. M., McCormick, J. E., and Feeney, J. (2000) *Biochemistry 39*, 15920−15931.
29. Sklenar, V., Piotto, M., Leppik, R., and Saudek, V. (1993) *J. Biomol. NMR A 102*, 241−245.
30. Cavanagh, J., Fairbrother, W. J., Palmer, A. G., III, and Skelton, N. J. (1996) *Protein NMR Spectroscopy*, Academic Press, New York.

31. Delaglio, F., Grzesiek, S., Vuister, G. W., Zhu, G., Pfeifer, J., and Bax, A. (1995) *J. Biomol. NMR 6*, 277−293.
32. Wishart, D. S., Bigam, C. G., Yao, J., Abildgaard, F., Dyson, H. J., Oldfield, E., Markley, J. L., and Sykes, B. D. (1995) *J. Biomol. NMR 6*, 135−140.
33. Bayley, P. M., Findlay, W. A., and Martin, S. R. (1996) *Protein Sci. 5*, 1215−1228.
34. Tjandra, N., Kuboniwa, H., Ren, H., and Bax, A. (1995) *Eur. J. Biochem. 230*, 1014−1024.
35. Malmendal, A., Evenäs, J., Forsén, S., and Akke, M. (1999) *J. Mol. Biol. 293*, 883−899.
36. Urbauer, J. L., Short, J. H., Dow, L. K., and Wand, A. J. (1995) *Biochemistry 34*, 8099−8109.
37. Biekofsky, R. R., Martin, S. R., Browne, J. P., Bayley, P. M., and Feeney, J. (1998) *Biochemistry 37*, 7617−7629.
38. Yamazaki, T., Otomo, T., Oda, N., Kyogoku, Y., Uegaki, K., Ito, N., Ishino, Y., and Nakamura, H. (1998) *J. Am. Chem. Soc. 120*, 5591−5592.
39. Xu, R., Ayers, B., Cowburn, D., and Muir, T. W. (1999) *Proc. Natl. Acad. Sci. U.S.A. 96*, 388−393.
40. Guex, N., and Peitsch, M. C. (1997) *Electrophoresis 18*, 2714−2723.

BI012187S